Title

Design, synthesis, and biological characterization of novel PEG-linked dimeric modulators for CXCR4

Journal

Bioorganic & Medicinal Chemistry, 24(21)

ISSN

0968-0896

Authors

Yang, Yilei
Gao, Mei
Zhang, Qinghao
et al.

Publication Date

2016-11-01

DOI

10.1016/j.bmc.2016.08.062

Peer reviewed

HHS Public Access

Author manuscript

Bioorg Med Chem. Author manuscript; available in PMC 2017 July 05.

Published in final edited form as:

Bioorg Med Chem. 2016 November 01; 24(21): 5393–5399. doi:10.1016/j.bmc.2016.08.062.

Design, synthesis, and biological characterization of novel PEG-linked dimeric modulators for CXCR4

Yilei Yang[a,b,†], **Mei Gao**[a,†], **Qinghao Zhang**[a], **Xiaohong Yang**[b], **Ziwei Huang**[c,*], and **Jing An**[a,c,*]

[a]Department of Pharmacology, Upstate Medical University, State University of New York (SUNY), 750 Adams Street, Syracuse, NY 13210, USA

[b]School of Pharmaceutical Sciences, Jilin University, Changchun, Jilin 130021, China

[c]Department of Medicine, University of California at San Diego, 9500 Gilman Drive, CA 92093

Abstract

CXCR4 dimerization has been widely demonstrated both biologically and structurally. This paper mainly focused on the development of structure-based dimeric ligands that target SDF-1α-CXCR4 interaction and signaling. This study presents the design and synthesis of a series of [PEG]n ([-CH_2-CH_2-O-]n) linked dimeric ligands of CXCR4 based on the knowledge of the homodimeric crystal structure of CXCR4 and our well established platform of chemistry and bioassays for CXCR4. These new ligands include $[PEG]_n$ linked homodimeric or heterodimeric peptides consisting of either two DV3-derived moieties (where DV3 is an all-D-amino acid analog of N-terminal modules of 1–10 (V3) residues of vMIP-II) or hybrids of DV3 moieties and SDF-$1\alpha_{1-8}$. Among a total of 24 peptide ligands, four antagonists and three agonists showed good CXCR4 binding affinity, with IC_{50} values of <50 nM and <800 nM, respectively. Chemotaxis and calcium mobilization assays with SUP-T1 cells further identified two promising lead modulators of CXCR4: ligand **4**, a $[PEG_3]_2$ linked homodimeric DV3, was an effective CXCR4 antagonist (IC_{50} = 22 nM); and ligand **21**, a $[PEG_3]_2$ linked heterodimeric DV3–SDF-$1\alpha_{1-8}$, was an effective CXCR4 agonist (IC_{50} = 407 nM). These dimeric CXCR4 modulators represent new molecular probes and therapeutics that effectively modulate SDF-1α-CXCR4 interaction and function.

Keywords

CXCR4; PEG; dimeric ligands

1. Introduction

The CXC chemokine receptor 4 (CXCR4) is a G-protein-coupled receptor. It consists of 352 amino acid residues that comprise an amino (N)-terminus, three extracellular and intracellular loops, seven transmembrane (TM) helices, and a carboxyl (C)-terminus [1–3].

To whom correspondence should be addressed. Tel.: (858) 822-0333; Fax: (858) 822-3344; zhuang@ucsd.edu (Z. Huang). Tel.: (315) 464-7952; Fax: (315) 464-0814; jan@ucsd.edu (J An).

†YY and MG contributed equally to this paper

CXCR4 transmits signals from extracellular ligands to intracellular biological pathways upon binding with its natural ligand, stromal-cell derived factor (SDF)-1α [4–6]. The SDF-1α-CXCR4 axis plays an important role in the regulation of leukocyte chemotaxis, angiogenesis, cancer metastasis, and HIV-1 infection [7–11].

Recently reported crystal structures of CXCR4 have revealed the importance of CXCR4 homodimerization or heterodimerization (with other GPCRs) in CXCR4 functions [2]. A two-site model for separation of binding and signaling is assumed, based on chimeric, mutational, and crystal studies [2, 12]. The binding pocket of CXCR4 is located close to the extracellular surface, as indicated by the co-crystal structures of CXCR4 bound to an antagonistic small molecule (IT1t), a cyclic peptide (CVX15), and vMIP-II [2, 12]. This pocket includes the acidic residues Asp^{187}, Glu^{288}, and Asp^{97}, which are critical for SDF-1α binding [2, 13, 14]. The importance of Glu^{288} for inhibition of SDF-1α signaling and HIV entry mediated by synthetic CXCR4 antagonist ligands (e.g., DV1) was also demonstrated in our previous research [6, 14, 15]. The N-terminus of SDF-1α may use the sequence motif that occurs immediately after the first two cysteine residues to interact with the extracellular loops of CXCR4, thereby reaching deeper into the transmembrane domains of CXCR4 for signaling. Conjugation of low-affinity peptides derived from the N-terminal sequence of SDF-1α with the stable and high-affinity CXCR4 antagonist confers agonist properties to the hybrid peptides, which retain high binding activity [16]. Further deciphering of the structure-function details of CXCR4 with its synthetic ligands will generate new opportunities for drug discovery efforts that target specific functional residues of this receptor.

In addition to its endogenous ligands, CXCR4 can be recognized by an extraneous viral derived antagonistic ligand, named viral macrophage inflammatory protein-II (vMIP-II) [13]. This vMIP-II ligand is encoded by the Kaposi's sarcoma-associated herpes virus and displays a broad spectrum of receptor-binding activities when compared to native chemokines, as it binds with high affinity to a number of both CC and CXC chemokine receptors, such as CCR5 and CXCR4 [17–19]. In the past several years, we have successfully transformed vMIP-II, a very nonselective chemokine, into a series of new analogs with significantly enhanced selectivity and potency for CXCR4, through modifications of only small N-terminal modules of 1–21 (V1) and 1–10 (V3) residues [20–22]. An all-D-amino acid analog of the V1 peptide, DV1, displays higher binding affinity than V1 for CXCR4 [23]. The turn-like, hydrophobic structure of DV1, consisting of Trp^5, His^6, and Pro^8 residues, which is critical for selective CXCR4 binding. Leu1 exhibits hydrophobic interactions with His113, Val114, and Ile259 of CXCR4; Ser4 forms a hydrogen bond with Tyr28 of CXCR4; and His6 undergoes van der Waals interactions with Ile269 of CXCR4 [22, 24]. We conjugated DV1 with its 10 N-terminal D-amino acid residues (named DV3) and generated a new dimeric ligand DV1-K-DV3. This new dimeric analog showed higher affinity for CXCR4 and effective anti-HIV activity [25]. It also selectively lost its capability to bind to other receptors (e.g., CXCR5). The use of unnatural D-peptides can be advantageous for molecular probe and therapeutic development, because these D-peptides are highly stable under physiological conditions [21–24].

In the present study, we used knowledge of the homodimeric crystal structure of CXCR4 [2] and Fmoc solid-phase chemistry to design and synthesize a series of PEG linked homodimeric or heterodimeric peptides consisting of either two DV3-derived moieties or hybrids of DV3 moieties and SDF-1α(1–8), according to the methods published previously [26–30]. We developed two promising modulators of CXCR4: one homodimeric peptide that was an effective antagonist and one heterodimeric peptide was an effective agonist. The process for synthesizing these new dimeric CXCR4 modulators was simpler and more rapid than that for the DV1 dimers, but they showed considerable biological activity. They represent new probes and drug candidates for regulation of CXCR4 function.

2. Results and discussion

2.1. Identification of high affinity dimeric ligands for CXCR4

We synthesized a series of new dimeric CXCR4 ligands using PEGn as a linker (Chart 1, Schemes 1 & 2). The two wild-type $(DV3)_2$ linked by PEG_3, PEG_5, and PEG_7 had similar IC_{50} values: $(DV3\text{-}PEG_3)_2K$ (**4**) (IC_{50}=22 nM), $(DV3\text{-}PEG_5)_2K$ (**5**) (IC_{50}=23 nM), and $(DV3\text{-}PEG_7)_2K$ (**6**) (IC_{50}=25 nM) (Figure 1, Table 1). This finding suggests that the length of PEG3 is optimal and that any length longer than PEG_3 is redundant for the function of dimeric DV3. We calculated the distance between two binding sites of dimeric CXCR4 as 40 angstroms. The linker of peptide 4 in the modeling analysis has nearly the same distance of 40 angstroms. The $(DV3\text{-}PEG_3)_2K$ (**4**) had similar CXCR4 binding affinity to that of AMD3100 (IC_{50}=65 nM); but its binding dramatically higher than the following controls: the DV3 monomer (**1**) (IC_{50}=2 μM); the short linker lysine linked DV3 dimer (**2**) (IC_{50}=462 nM); and the monomer $DV3\text{-}PEG_3\text{-}K$ (**3**) (IC_{50} = 2.2 μM). The lowering or reduction of CXCR4 binding affinity caused by the deletion of amino acids of $DV3_{4–10}$ (**7–14**) indicated the importance of these amino acids. An increase in the length of the PEG linkers (**10–14**) to compensate for the deletions of the C-terminal $DV3_{4–10}$ (to keep the total linear length of dimer peptide unchanged) did not restore or increase the CXCR4 binding affinity (Table 1 and Figure 1). The importance of the last four C-terminal amino acids of DV3 was further confirmed by synthesizing new analogs using an alanine scanning mutagenesis strategy. Single amino acid mutations of $DV3_{7–10}$ (**15–18**) showed that $DV3_7$ and $DV3_{10}$ mutation resulted in a decrease in the CXCR4 binding affinity, $DV3_8$ and $DV3_9$ mutation did not show significant change of CXCR4 binding affinity (Table 1) and cell migration (Table 2, see 3.3.) activity.

In contrast to the monomer DV3, the N-terminal SDF-1α derived monomer peptide $SDF\text{-}1α_{1–8}$ (**19**) showed a very low CXCR4 binding affinity. We employed the same PEG linker strategy to synthesize a number of PEG linked heterodimeric peptide ligands of CXCR4: **21** [$DV3\text{-}PEG_3\text{-}K\text{-}(PEG_3\text{-}SDF\text{-}1α_{1–8})$], **22** [$DV3\text{-}PEG_5\text{-}K\text{-}(PEG_5\text{-}SDF\text{-}1α_{1–8})$], **22** [$DV3\text{-}PEG_3\text{-}K\text{-}(PEG_3\text{-}SDF\text{-}1α_{1–5})$], and **24** [$DV3\text{-}PEG_3\text{-}K\text{-}(PEG_5\text{-}SDF\text{-}1α_{1–6})$] (Table 1). Ligand **21** exhibited the best CXCR4 binding and agonist (**see 3.2 & 3.3**) activity of all the other ligands, as defined by the calcium mobilization assay and migration assay.

2.2. Characterization of lead dimeric ligands of CXCR4 that mediate Ca^{2+} signaling

The interaction of CXCR4 with its ligands can trigger a series of intracellular signaling pathways. Among these, the Ca^{2+} mobilization mediated signaling is very critical and typically involved in SDF-1α/CXCR4 mediated chemotaxis. We conducted intracellular Ca^{2+} influx experiments in order to identify lead ligands that had either antagonist or agonist activity using Synergy H1 with a Ca^{2+} indicator, Fura-2/AM. Based on CXCR4 binding studies, we performed a series of primary $Ca2^{+}$ influx assays for both peptides and their analogs; these showed good CXCR4 binding activities in the absence and presence of SDF-1α, respectively. We selected the following candidate peptide ligands: **4–7**, **16**, and **17**, which were homodimeric CXCR4 ligands and **20–22** and **24**, which were heterodimeric ligands. We found that ligand **4** had only antagonistic activity and ligand **21** had only agonistic activity (Figure 2). Ligand **4** at 1 μM and 200 nM, inhibited approximately 90% and 50% Ca^{2+} influx caused by 100 nM SDF-1α stimulation, respectively (Figure 2A). Other homodimeric ligands, including **5–7**, **16**, and **17**, showed weaker or slightly antagonistic effects on the SDF-1α-induced Ca^{2+} influx.

In contrast, ligand **21** at 2 μM triggered a Ca^{2+} influx as strong as that seen in response to 100 nM SDF-1α. Under the same experimental condition, ligand **21** at 400 nM was sufficient to trigger 50% of the Ca^{2+} influx induced by 100 nM SDF-1α (Figure 2B). Ligand **20** showed a weaker agonistic effect on Ca^{2+} influx, while ligands **22–24** showed no significant effect (data not shown).

2.3. Evaluation of $CXCR4^{+}$ cell migration mediated by dimeric ligands

We further confirmed the antagonist and agonist activity of these lead CXCR4 ligands by performing cell migration assays in the presence or absence of SDF-1α. Ligand **4** showed the highest inhibitory activity against migration of $CXCR4^{+}$ SUP-T1 cells: at 100 nM it inhibited more than 65% of the cell migration triggered by 10 nM SDF-1α. By contrast, Ligands **6, 7**, **10**, **16,** and **17** inhibited cell migration in response to 10 nM SDF-1α treatment by less than 50%, indicating that the PEG_3 linked dimer DV3 (ligand **4**) is the lead antagonist candidate for CXCR4 (Figure 3A). We checked the effects of these peptides on cell viability at 100 nM; none of the peptides showed any cytotoxic effects on these cells.

The reduced antagonist activity of ligands **6, 7**, **16,** and **17** suggests that the full sequence of DV3 (1–10 amino acids), the $(PEG_3)_2$ linker, and the 8^{th} and 9^{th} amino acids are all critical for the antagonist function of ligand **4**. Ligand **5** showed similar anti-migration activity to ligand **4**, but the ligand **6** with longer linker $(PEG_7)_2$ showed weaker anti-migration activity than ligand **3** (Table 2) and therefore made it less ideal for future modification and application.

Among the heterodimeric ligands **20–22** and **24,** the PEG_3 linked heterodimeric ligand **21** showed good activity for promoting $CXCR4^{+}$ SUP-T1 migration (Figure 3B), which is consistent with its Ca^{2+} influx assay results.

3. Conclusions

In conclusion, we used a dual-motif strategy to design and synthesize a series of new PEG-linked dimeric DV3 [e.g., $(DV3\text{-}PEG_3)_2K$] analogs. We demonstrated potent binding activities of PEG-linked homo- or heterodimerized DV3 analogs that were dependent on the DV3 dual motif, the amino acid sequences, and the length of PEG linkers. We confirmed that these novel CXCR4 modulators have extremely potent activity at low nanomolar concentrations and can block (homodimeric analogs) or promote (heterodimeric analogs) Ca^{2+} influx-mediated signaling and the chemotactic migration of CXCR4-expressing cells. Two promising modulators of CXCR4 were identified: one homodimeric peptide **4** $(DV3\text{-}PEG_3)_2K$ was an effective antagonist, and one heterodimeric peptide **21** $DV3\text{-}PEG_3\text{-}K\text{-}(PEG_3\text{-}SDF\text{-}1\alpha_{1–8})$ was an effective agonist. These dimeric CXCR4 modulators may be valuable in developing new probes and experimental therapeutics that target SDF-1α-CXCR4 interaction and function.

4. Experimental section

4.1. Chemistry

All crude peptides were purified by RP-HPLC with the gradients of acetonitrile in water containing 0.01% TFA. The purity (>95%) of all peptides was checked by analytical HPLC through a C18 reverse-phase column (Figures S1 and S2), while the molecular weights of peptides were determined by MALDI-TOF-MS (Table S1). The monomer peptides **1**, **19,** and dimer peptide **2** were synthesized according to a common Fmoc solid-phase peptide synthesis method published previously (14, 21, 23). The peptide **3** was purchased from Crefu Peptides (Shanghai, China).

4.2. Synthesis of homodimer peptide 4–18

The Rink amide resin (1 equiv) was added to the reaction container, washed with DCM and DMF, and deprotected twice with 20% piperidine in DMF for 10 min each time. The Fmoc-Lys(Fmoc)-OH (5 equiv), HOBt (5 equiv) and DIC (5 equiv) were added together with 2 mL DMF and reacted for 4 h, The two Fmoc groups of lysine were deprotected and coupled with different linker (10 equiv) together with HOBt (10 equiv) and DIC (10 equiv) in 2 mL DMF for 6 h. Fmoc-NH-$(PEG)_mCH_2CH_2$-COOH (MW=443.50) was used to synthesized peptides **4–18**. Different lengths of the DV3 sequence, from the C-terminal to the N-terminal, were then coupled onto the PEG linker through Fmoc-D-aa by the same method used for coupling of the linker. For peptides **15**, **16**, **17,** and **18**, the amino acid of DV3 at position 7, 8, 9, and 10 was mutated into alanine, respectively.

The Fmoc groups of last amino acids acid was deprotected, and the peptide was then cleaved from the resin with the cocktail cleavage solution (TFA:H_2O:Thiophenol = 90:5:5). The crude peptide was precipitated and washed twice with cold ethyl ether.

4.3. Synthesis of heterodimer peptide 20–24

The Rink amide resin (1 equiv) was washed with DCM and DMF in the reaction container, and deprotected twice with 20% piperidine in DMF for 10 min each time. The Fmoc-

Lys(dde)-OH (5 equiv), HOBt (5 equiv) and DIC (5 equiv) were coupled with resin in 2 mL DMF for 4 h. For peptides **21–24**, one PEG linker was coupled to the N-α position of the first lysine using Fmoc-NH-$(PEG)_3CH_2CH_2$-COOH (MW=443.50). The DV3 sequence from the C-terminal to the N-terminal was coupled onto the PEG linker with the last D-amino acid protected by Boc group. After the coupling of the DV3 sequence was complete, the dde group of the first coupled lysine was deprotected with 2% hydrazine in DMF. Then, the other PEG linker was coupled onto the ε-amino group of the first coupled lysine and the sequence of SDF-$1\alpha_{1-8}$ from the C-terminal to N-terminal was coupled onto the PEG linker through Fmoc-L-aa (5 equiv), HOBt (5 equiv) and DIC (5 equiv) in 2 mL DMF. For peptide **20**, the DV3 and SDF-$1\alpha_{1-8}$ sequences was directly coupled to the α and ε amino groups of the first lysine, respectively. The Fmoc groups of last amino acids acid was deprotected before washing with DMF and DCM, then the peptide was cleaved from the resin with a cocktail cleavage solution (TFA:H_2O:Thiophenol=90:5:5) for 2 h. The crude peptide was precipitated and washed twice with cold ethyl ether.

4.4. Competitive CXCR4 binding assay

CHO cells stably transfected with CXCR4 (over 98% CXCR4-positive cells) were cultured in RPMI1640 medium with 10% (v/v) FBS, 100 IU penicillin, 0.1 mg/mL streptomycin and 2 mM L-glutamine. Cells were collected and washed twice with FACS buffer (0.5% BSA, 0.05% sodium azide in phosphate-buffered saline). Competition binding experiments were performed using anti-CXCR4 MAb (1:2000, mouse anti-human CD184 antibody, BD Biosciences, USA) in a final volume of 100 μL FACS buffer containing 4×10^5 cells in V-shaped 96-well plates in the presence of various concentrations of peptides. After incubation for 40 min at 4°C, cells were washed twice with FACS buffer, and then were stained with anti-mouse IgG-FITC (1: 1000, Sigma, St. Louis, MO) for 30 min at 4°C. As a negative control, cells were stained only with the secondary antibody. The cells were washed with FACS buffer and resuspended in 100 μL of FACS buffer before the fluorescence (485_{EX}/528_{EM}) was analyzed on a Synergy 2 microplate reader (BioTek, USA). At least three independent experiments were performed. The binding data were analyzed using GraphPad Prism 5. All data are shown as means ± S.E. from at least three independent experiments.

4.5. Calcium mobilization assay

SUP-T1 cells were collected and washed twice with Hank's balanced salt saline solution [140 mM NaCl, 5 mM KCl, 10 mM Hepes (pH 7.4), 1 mM $CaCl_2$, 1 mM $MgCl_2$, 1 mg/mL glucose, and 0.025% BSA]. The cells (10^7 cells/mL) were then loaded with fura-2/AM (2 μM, Molecular Probes, USA) and probenecid sodium (5 μM, Sigma, USA) in the same buffer for 30 min in a 5% CO_2 incubator with gentle vortexing every 5 min. After incubation, the cells were washed and resuspended at a density of 2×10^6 cells/mL. A 200 μL volume of cells were then added per well to a 96-well opaque black plate. Fura-2 fluorescence was measured on a Synergy H1 microplate reader (BioTek, USA) using excitation wavelength of 340 and 380 nm and an emission wavelength of 510 nm. The antagonist activity was evaluated by pre-incubating the peptides with cells for 2–3 min, followed by stimulation with 50 nM SDF-1α. The agonist activity was evaluated by adding the peptides to the cells after recording the base line for 2 min.

4.6. CXCR4 chemotaxis assay

SUP-T1 cells were cultured in RPMI1640 medium with 10% (v/v) FBS, 100 IU penicillin, 0.1 mg/mL streptomycin, and 2 mM L-glutamine. On the day of experiment, the cells were collected and washed twice with assay buffer (RPMI1640 medium with 0.5% BSA) by centrifugation. For antagonist assay, a sample containing 1×10^6 cells was first incubated with peptides of various concentrations for 2 h, and then were seeded at 100 μl per well in the upper chambers of HTS transwell 96-well plates with 5 μm pore size (Corning, USA). The upper chambers were placed into the lower chambers, which contained 200 μL assay buffer and 10 nM SDF-1α as chemoattractant. Background groups were run by adding only assay buffer to the lower chambers. For agonist assay, peptides were added into 200 μL assay buffer in lower chamber at different concentrations and 10 nM SDF-1α was used as a positive control. The transwell plate was placed in a 37°C cell culture incubator for 3 h while the cells were allowed to migrate. After incubation, the upper chambers were removed and SUP-T1 cells that had migrated to the lower chambers were quantified by Cell Titer-Blue reagent (Promega, USA).

Acknowledgments

This work was supported by the grant GM057761 from the National Institutes of Health. Y. Y. was supported in part by the Chinese Scholarship Council.

References

1. Berger EA, Murphy PM, Farber JM. Chemokine receptors as HIV-1 coreceptors: roles in viral entry, tropism, and disease. Annu Rev Immunol. 1999; 17:657. [PubMed: 10358771]
2. Wu B, Chien EY, Mol CD, Fenalti G, Liu W, Katritch V, Abagyan R, Brooun A, Wells P, Bi FC, Hamel DJ, Kuhn P, Handel TM, Cherezov V, Stevens RC. Structures of the CXCR4 chemokine GPCR with small-molecule and cyclic peptide antagonists. Science. 2010; 330:1066. [PubMed: 20929726]
3. Nichols S, Hernández; CX, Wang Y, McCammon JA. Structure-based network analysis of an evolved G protein-coupled receptor homodimer interface. Protein Sci. 2013; 22:745. [PubMed: 23553730]
4. Premack BA, Schall TJ. Chemokine receptors: gateways to inflammation and infection. Nature Med. 1996; 2:174.
5. Choi WT, Tian S, Dong CZ, Kumar S, Liu D, Madani N, An J, Sodroski JG, Huang Z. Unique ligand binding sites on CXCR4 probed by a chemical biology approach: implications for the design of selective human immunodeficiency virus type 1 inhibitors. J Virol. 2005; 79:15398. [PubMed: 16306611]
6. Tian S, Choi WT, Liu D, Pasavento J, Wang Y, An J, Sodroski JG, Huang Z. Distinct functional sites for human immunodeficiency virus type 1 and stromal cell-derived factor 1α on CXCR4 transmembrane helical domains. J Virol. 2005; 79:12667. [PubMed: 16188969]
7. Zlotnik A, Yoshie O. Chemokines: a new classification system and their role in immunity. Immunity. 2000; 12:121. [PubMed: 10714678]
8. Muller A, Homey B, Soto H, Ge NF, Catron D, Mohar A, Verastegui E, Zlotnik A. Involvement of ckemokine receptors in breast cancer metastasis. Nature. 2001; 410:50. [PubMed: 11242036]
9. Patrussi L, Baldari CT. Intracellular mediators of CXCR4-dependent signaling in T cells. Immunol Lett. 2008; 115:75. [PubMed: 18054087]
10. Liekens S, Schols D, Hatse S. CXCL12-CXCR4 axis in angiogenesis, metastasis and stem cell mobilization. Curr Pharm Des. 2010; 16:3903. [PubMed: 21158728]

11. Choi WT, Yang Y, Xu Y, An J. Targeting chemokine receptor CXCR4 for treatment of HIV-1 infection, tumor progression, and metastasis. Curr Top Med Chem. 2014; 14:1574. [PubMed: 25159167]
12. Percherancier Y, Berchiche YA, Slight I, Volkmer-Engert R, Tamamura H. Bioluminescence resonance energy transfer reveals ligand-induced conformational changes in CXCR4 homo- and heterodimers. J Biol Chem. 2005; 280:9895. [PubMed: 15632118]
13. Qin L, Kufareva I, Holden LG, Wang C, Zheng Y, Zhao C, Fenalti G, Wu H, Han GW, Cherezov V, Abagyan R, Stevens RC, Handel TM. Structural biology. Crystal structure of the chemokine receptor CXCR4 in complex with a viral chemokine. Science. 2015; 347:1117. [PubMed: 25612609]
14. Choi W, Santhosh K, Madani N, Han X, Tian S, Dong C, Liu D, Duggineni S, Yuan J, Sodroski JG, Huang Z, An J. A novel synthetic bivalent ligand to probe chemokine receptor CXCR4 dimerization and inhibit HIV-1 entry. Biochemistry. 2012; 51:7078. [PubMed: 22897429]
15. Dong CZ, Kumar S, Choi WT, Madani N, Tian S, An J, Sodroski JG, Huang Z. Different stereochemical requirements for CXCR4 binding and signaling functions as revealed by an anti-HIV, D-amino acid-containing SMM-chemokine ligand. J Med Chem. 2005; 48:7923. [PubMed: 16335916]
16. Lefranc-ois M, Lefebvre M, Saint-Onge G, Boulais PE, Lamothe S, Leduc R, Lavigne P, Heveker N, Escher E. Agonists for the chemokine receptor CXCR4. ACS Med Chem Lett. 2011; 2:597. [PubMed: 21841963]
17. Moore PS, Boshoff CE, Weiss RA, Chang Y. Molecular mimicry of human cytokine and cytokine response pathway genes by KSHV. Science. 1996; 274:1739. [PubMed: 8939871]
18. Boshoff CEY, Collins PD, Takeuchi Y, Reeves JD, Schweickart VL, Siani MA, Sasaki T, Williams TJ, Gray PW, Moore PS, Chang Y, Weiss RA. Angiogenic and HIV-inhibitory functions of KSHV-encoded chemokines. Science. 1997; 278:290. [PubMed: 9323208]
19. Kledal TN, Rosenkilde MM, Coulin F, Simmons G, Johnsen AH, Alouani S, Power CA, Luttichau HR, Gerstoft J, Clapham PR, Clark-Lewis I, Wells TNC, Schwartz TW. A broad-spectrum chemokine antagonist encoded by Kaposi's sarcoma-associated herpesvirus. Science. 1997; 277:1656. [PubMed: 9287217]
20. Luo Z, Fan X, Zhou N, Hiraoka M, Luo J, Kaji H, Huang Z. Structure-function study and anti-HIV activity of synthetic peptide analogues derived from viral chemokine vMIP-II. Biochemistry. 2000; 39:13545. [PubMed: 11063591]
21. Kumar S, Choi WT, Dong CZ, Madani N, Tian S, Liu D, An J, Sodroski JG, Richman DD, Huang Z. SMM-chemokines: a class of unnatural synthetic molecules as chemical probes of chemokine receptor biology and leads for therapeutic development. Chem Biol. 2006; 13:69. [PubMed: 16426973]
22. Liu D, Madani N, Li Y, Cao R, Choi WT, Kawatkar SP, Lim MY, Kumar S, Dong CZ, Wang J, Russell JD, Lefebure CR, An J, Wilson S, Gao YG, Pallansch LA, Sodroski JG, Huang Z. Crystal structure and structural mechanism of a novel anti-human immunodeficiency virus and D-Amino acid-containing chemokine. J Virol. 2007; 81:11489. [PubMed: 17686848]
23. Zhou N, Luo Z, Luo J, Fan X, Cayabyab M, An J, Kaji H, Sodroski JG, Huang Z. Exploring the stereochemistry of CXCR4-peptide recognition and inhibiting HIV-1 entry with D-peptides derived from chemokines. J Biol Chem. 2002; 277:17476. [PubMed: 11880384]
24. Mori M, Liu D, Kumar S, Huang Z. NMR structures of anti-HIV D-peptides derived from the N-terminus of viral chemokine vMIP-II. Biochem Biophys Res Commun. 2005; 335:651. [PubMed: 16115468]
25. Xu Y, Duggineni S, Espitia S, Richman DD, An J, Huang Z. A synthetic bivalent ligand of CXCR4 inhibits HIV infection. Biochem Biophys Res Commun. 2013; 435:646. [PubMed: 23688427]
26. Kühhorn J, Hübner H, Gmeiner P. Bivalent Dopamine D2 Receptor ligands: synthesis and binding properties. J Med Chem. 2011; 54:4896. [PubMed: 21599022]
27. Kühhorn J, Gŏtz A, Hübner H, Thompson D, Whistler J, Gmeiner P. Development of a bivalent dopamine D2 receptor agonist. J Med Chem. 2011; 54:7911–7919. [PubMed: 21999579]

28. Zhang B, Zhang T, Sromek AW, Scrimale T, Bidlack JM, Neumeyer JL. Synthesis and binding affinity of novel mono- and bivalent morphinan ligands for κ, μ and δ opioid receptors. Bioorg Med Chem. 2011; 19:2808. [PubMed: 21482470]

29. Handl HL, Sankaranarayanan R, Josan JS, Vagner J, Mash EA, Gillies RJ, Hruby VJ. Synthesis and Evaluation of Bivalent NDP-α-MSH(7) Peptide ligands for binding to the human melanocortin receptor 4 (hMC4R). Bioconjugate Chem. 2007; 18:1101.

30. Tanaka T, Nomura W, Narumi T, Masuda A, Tamamura H. Bivalent ligands of CXCR4 with rigid linkers for elucidation of the dimerization state in cells. J Am Chem Soc. 2010; 132:15899. [PubMed: 20973474]

31. Biernat M, Stefanowicz P, Zimecki M, Szewczuk Z. Amino-terminal dimerization of peptides on the solid support. synthesis and biological activity of the immunosuppressive HLA-DR fragments linked by poly(ethylene glycol)s. Bioconjugate Chem. 2006; 17:1116.

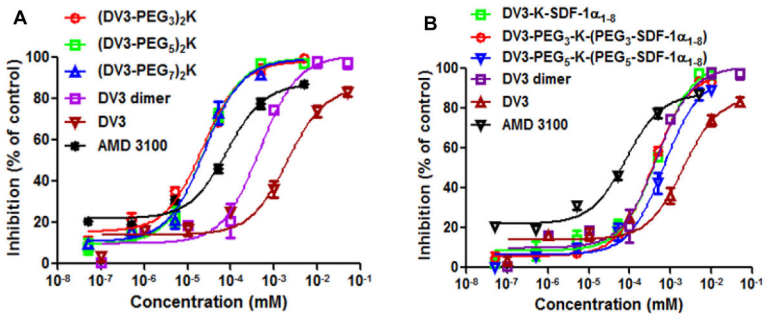

Figure 1.

A. Comparison of the CXCR4 binding activity of PEG linked DV3 homodimers. B. Comparison of the CXCR4 binding activity of PEG linked DV3 and SDF-1α_{1-8} heterodimers. The IC_{50} values of these ligands were determined by 12G5 antibody competitive binding assays (Table 1). All data are presented as mean ± S.E. from at least three independent experiments.

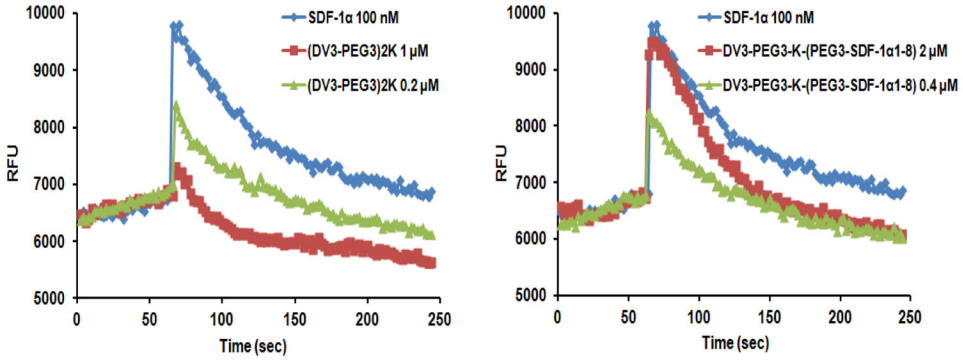

Figure 2.

Effects of PEG-linked DV3 analogs on CXCR4-mediated calcium mobilization. Ca^{2+} influx in SUP-T1 cells was measured in response to the treatment with SDF-1α and/or DV3 analogs. For antagonistic assay (A), peptides were pretreated for 3 min before SDF-1α was added into the cells; for agonistic assay (B), peptides were added in the same pattern as SDF-1α.

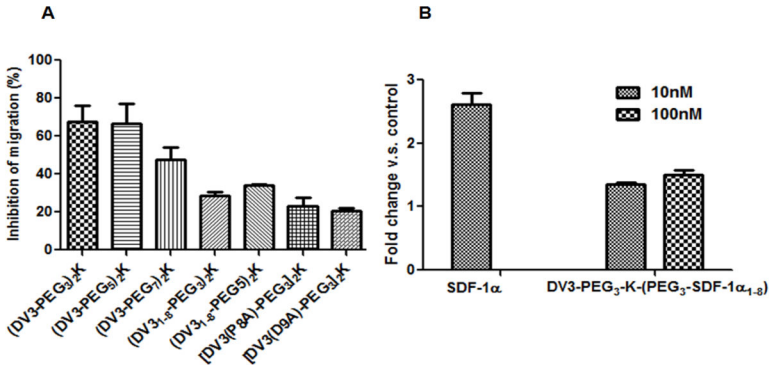

Figure 3.

Effects of PEG-linked DV3 analogs on CXCR4-dependent chemotaxis. A. The antagonist activity of homodimeric peptides (100 nM) in blocking SDF-1α-mediated chemotaxis. Chemotaxis was expressed as the percentage of SUP-T1 cells initially seeded in the transwells that migrated into the bottom chambers following stimulation by 10 nM SDF-1α. B. The agonist activity of chemotaxis induced by heterodimeric peptides that mimics SDF-1α-mediated chemotaxis. Data were expressed as the fold change of migrated SUP-T1 cells into the bottom chambers following stimulated with 10 nM SDF-1α or heterodimeric ligand **21** compared with vehicle group. Each experimental data point was generated from at least three independent experiments and expressed as mean ± S.E.

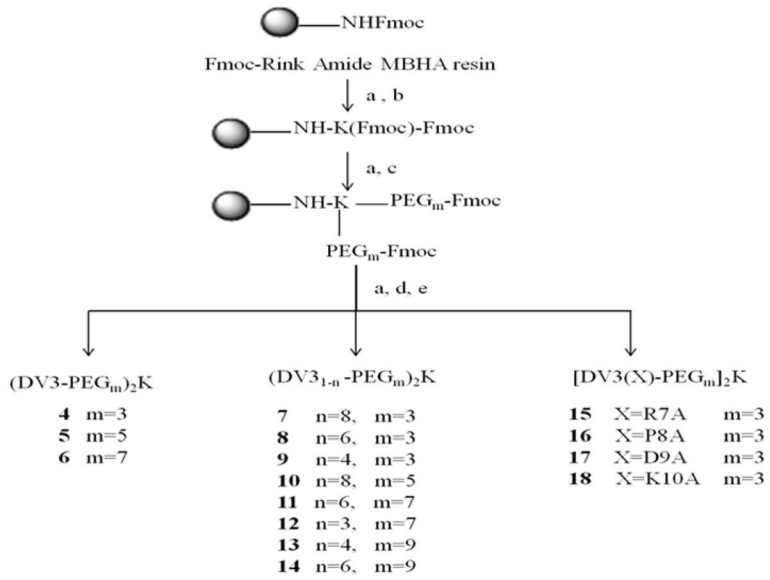

Scheme 1.

Scheme of solid-phase synthesis of homodimer peptide ligands of 4–18. Reagents and conditions: (a) 20% piperidine in DMF. (b) Fmoc-Lys(Fmoc)-OH, HOBt, DIC and DMF. (c) Fmoc-NH-(PEG)m-CH_2CH_2-COOH, HOBt, DIC and DMF. (d) Fmoc-D-aa, HOBt, DIC and DMF. (e) TFA:H_2O:Thiophenol = 90:5:5.

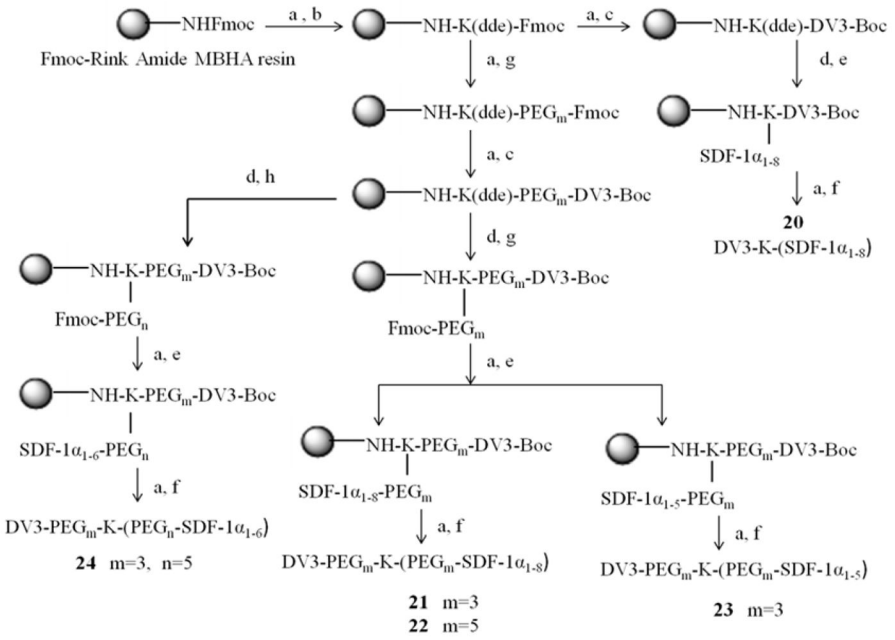

Scheme 2.

Scheme of solid-phase synthesis of heterodimer peptide ligands of 20–24. Reagents and conditions: (a) 20% piperidine in DMF. (b) Fmoc-Lys(dde)-OH, HOBt, DIC and DMF. (c) Fmoc-D-aa, HOBt, DIC and DMF. (d) 2% hydrazine in DMF. (e) Fmoc-L-aa, HOBt, DIC and DMF. (f) TFA:H_2O:Thiophenol = 90:5:5. (g) Fmoc-NH-$(PEG)_mCH_2CH_2$-COOH, HOBt, DIC and DMF. (h) Fmoc-NH-$(PEG)_nCH_2CH_2$-COOH, HOBt, DIC and DMF.

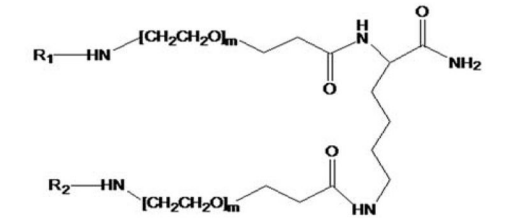

R_1=R_2=DV3, m=3, **4**
R_1=R_2=DV3, m=5, **5**
R_1=R_2=DV3, m=7, **6**
R_1=R_2=$DV3_{1-8}$, m=3, **7**
R_1=R_2=$DV3_{1-6}$, m=3, **8**
R_1=R_2=$DV3_{1-4}$, m=3, **9**
R_1=R_2=$DV3_{1-8}$, m=5, **10**
R_1=R_2=$DV3_{1-6}$, m=7, **11**
R_1=R_2=$DV3_{1-3}$, m=7, **12**
R_1=R_2=$DV3_{1-4}$, m=9, **13**
R_1=R_2=$DV3_{1-6}$, m=9, **14**
R_1=R_2=DV3(R7A), m=3, **15**
R_1=R_2=DV3(P8A), m=3, **16**
R_1=R_2=DV3(D9A), m=3, **17**
R_1=R_2=DV3(K10A), m=3, **18**
R_1=DV3, R_2= $SDF\text{-}1\alpha_{1-8}$, m=3, **21**
R_1=DV3, R_2= $SDF\text{-}1\alpha_{1-8}$, m=5, **22**
R_1=DV3, R_2= $SDF\text{-}1\alpha_{1-5}$, m=3, **23**

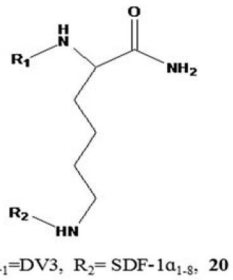

R_1=DV3, R_2= $SDF\text{-}1\alpha_{1-8}$, **20**

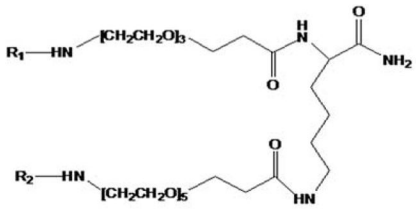

R_1=DV3, R_2= $SDF\text{-}1\alpha_{1-6}$, **24**

Chart 1.
Chemical structures of dimeric peptide ligands.

Table 1

The synthesized bivalent ligands and CXCR4 binding data.

No.	Peptide name	Structure[a,b]	CXCR4 binding activity(IC_{50})
1	DV3	**L-G-A-S-W-H-R-P-D-K**	2.0 ± 0.2 μM
2	DV3 dimer	**L-G-A-S-W-H-R-P-D-K** | **L-G-A-S-W-H-R-P-D-K**	462 ± 30.1 nM
3	DV3-PEG_3-K	**L-G-A-S-W-H-R-P-D-K**-PEG_3-K	2.2 ± 0.3 μM
4	$(DV3\text{-}PEG_3)_2K$	**L-G-A-S-W-H-R-P-D-K**-PEG_3-K | **L-G-A-S-W-H-R-P-D-K**-PEG_3	22 ± 1.2 nM
5	$(DV3\text{-}PEG_5)_2K$	**L-G-A-S-W-H-R-P-D-K**-PEG_5-K | **L-G-A-S-W-H-R-P-D-K**-PEG_5	23 ± 2.2 nM
6	$(DV3\text{-}PEG_7)_2K$	**L-G-A-S-W-H-R-P-D-K**-PEG_7-K | **L-G-A-S-W-H-R-P-D-K**-PEG_7	25 ± 2.9 nM
7	$(DV3_{1-8}\text{-}PEG_3)_2K$	**L-G-A-S-W-H-R-P**-PEG_3-K | **L-G-A-S-W-H-R-P**-PEG_3	144 ± 14.7 nM
8	$(DV3_{1-6}\text{-}PEG_3)_2K$	**L-G-A-S-W-H**-PEG_3-K | **L-G-A-S-W-H**-PEG_3	> 1 μM
9	$(DV3_{1-4}\text{-}PEG_3)_2K$	**L-G-A-S**-PEG_3-K | **L-G-A-S**-PEG_3	> 1 μM
10	$(DV3_{1-8}\text{-}PEG_5)_2K$	**L-G-A-S-W-H-R-P**-PEG_5-K | **L-G-A-S-W-H-R-P**-PEG_5	110 ± 14.2 nM
11	$(DV3_{1-6}\text{-}PEG_7)_2K$	**L-G-A-S-W-H**-PEG_7-K | **L-G-A-S-W-H**-PEG_7	> 1 μM
12	$(DV3_{1-3}\text{-}PEG_7)_2K$	**L-G-A**-PEG_7-K | **L-G-A**-PEG_7	> 1 μM
13	$(DV3_{1-4}\text{-}PEG_9)_2K$	**L-G-A-S**-PEG_9-K | **L-G-A-S**-PEG_9	> 1 μM

No.	Peptide name	Structure[a,b]	CXCR4 binding activity(IC_{50})
14	$(DV3_{1–6}\text{-}PEG_9)_2K$	**L-G-A-S-W-H-**PEG_9-K | **L-G-A-S-W-H-**PEG_9	> 1 μM
15	$[DV3(R7A)\text{-}PEG_3]_2K$	**L - G - A - S - W - H - A - P - D - K -** PEG_3 - K | **L - G - A - S - W - H - A - P - D - K -** PEG_3	> 1 μM
16	$[DV3(P8A)\text{-}PEG_3]_2K$	**L - G - A - S - W - H - R - A - D - K -** PEG_3 - K | **L - G - A - S - W - H - R - A - D - K -** PEG_3	64 ± 5.6 nM
17	$[DV3(D9A)\text{-}PEG_3]_2K$	**L - G - A - S - W - H - R - P - A - K -** PEG_3 - K | **L - G - A - S - W - H - R - P - A - K -** PEG_3	34 ± 4.2 nM
18	$[DV3(K10A)\text{-}PEG_3]_2K$	**L - G - A - S - W - H - R - P - D - A -** PEG_3 - K | **L - G - A - S - W - H - R - P - D - A -** PEG_3	> 1 μM
19	$SDF\text{-}1\alpha_{1–8}$	K-P-V-S-L-S-Y-R	No binding
20	$DV3\text{-}K\text{-}(SDF\text{-}1\alpha_{1–8})$	**L-G-A-S-W-H-R-P-D-K-**K | K-P-V-S-L-S-Y-R	502 ± 61.1 nM
21	$DV3\text{-}PEG_3\text{-}K\text{-}(PEG_3\text{-}SDF\text{-}1\alpha_{1–8})$	**L-G-A-S-W-H-R-P-D-K-**PEG_3-K | K-P-V-S-L-S-Y-R-PEG_3	407 ± 31.2 nM
22	$DV3\text{-}PEG_5\text{-}K\text{-}(PEG_5\text{-}SDF\text{-}1\alpha_{1–8})$	**L-G-A-S-W-H-R-P-D-K-**PEG_5-K | K-P-V-S-L-S-Y-R-PEG_5	747 ± 70.3 nM
23	$DV3\text{-}PEG_3\text{-}K\text{-}(PEG_3\text{-}SDF\text{-}1\alpha_{1–5})$	**L-G-A-S-W-H-R-P-D-K-**PEG_3-K | K-P-V-S-L-PEG_3	1.56 ± 0.2 μM
24	$DV3\text{-}PEG_3\text{-}K\text{-}(PEG_5\text{-}SDF\text{-}1\alpha_{1–6})$	**L-G-A-S-W-H-R-P-D-K-**PEG_3-K | K-P-V-S-L-S-PEG_5	737 ± 53.4 nM

[a] All bivalent ligands have an unmodified N-terminal and an amide modified C-terminal.

[b] All bold symbols are D-amino acids.

Table 2

Migration of $CXCR4^+$ cells mediated by homodimeric ligands.

No.	Peptide name	Migration activity (inhibition % at 100 nM)
4	$(DV3\text{-}PEG_3)_2K$	67 ± 8.2
5	$(DV3\text{-}PEG_5)_2K$	66 ± 9.3
6	$(DV3\text{-}PEG_7)_2K$	48 ± 5.9
7	$(DV3_{1-8}\text{-}PEG3)_2K$	28 ± 1.6
10	$(DV3_{1-8}\text{-}PEG_5)_2K$	34 ± 0.5
16	$[DV3(P8A)\text{-}PEG_3]_2K$	23 ± 3.6
17	$[DV3(D9A)\text{-}PEG_3]_2K$	21 ± 1.2